

Supporting Information

for

Paramagnetic Aluminum β -Diketiminate

by

Jani Moilanen, Javier Borau Garcia, Roland Roesler, and Heikki M. Tuononen*

1. Experimental details

All reactions and manipulations were performed under an argon atmosphere by using Schlenk techniques or an inert atmosphere glove box. Compounds MeAlCl₂ (1 M in hexanes, Aldrich) and *n*-BuLi (1.6 M in hexanes, Aldrich) were used as received. B(C₆H₅)₃ and B(C₆F₅)₃ (Aldrich) were dried with HMe₂SiCl and sublimed before use. CoCp*₂ and CoCp₂ (Aldrich) were sublimed before use. Compound **7** was prepared according to a literature procedure (*Eur. J. Org. Chem.*, 2004, 4319). All solvents were dried and deoxygenated prior to use. NMR spectra were recorded on a Bruker Avance 400 MHz or Bruker Avance II 300 MHz spectrometer. ¹H and ¹³C spectra were referenced to the residual solvent signal and the chemical shifts are reported relative to (CH₃)₄Si. Solutions of BF₃·Et₂O in C₆D₆ and neat C₆F₆ were used as internal references in ¹¹B and ¹⁹F measurements, respectively. The EPR spectrum of **4j** was recorded using an X-band Bruker EMX10/12 spectrometer. Elemental analyses were performed by Analytical Services at the Department of Chemistry, University of Calgary. Although the calculated and experimental data for the elemental analysis of both **9a** and **9b** deviate slightly (0.75 – 1.47%), the purity of the compounds is clearly shown by NMR spectroscopy (see below) as there are no ¹¹B- or ¹⁹F-containing impurities present in the sample. Consequently, we address the minor errors in elemental analysis to a small amount of H-grease present in the products.

8: A solution of **7** (681 mg, 4.0 mmol) in THF (10 ml) was cooled to -78 °C and *n*-BuLi (2.5 ml of a 1.6 M solution in hexane, 4.0 mmol) was added by syringe. The solution was stirred for 1 h at -78 °C and then warmed to -40 °C. MeAlCl₂ (2.0 ml of a 1 M solution in hexane, 2.0 mmol) was added by syringe and the solution was allowed to warm to ambient temperature over 1 h, after which it was warmed to 45 °C and stirred for additional 45 min. The hot solution was filtered and the solvents evaporated under vacuum. The residue was dissolved in CH₂Cl₂ (10 ml), filtered and the solvent was evaporated under vacuum. The solid residue was washed with hexane (2 x 10 ml) to afford **8** as an orange powder (430 mg, 57%). Crystallization from CH₂Cl₂ yielded orange single crystals suitable for X-ray analysis (see below). ¹H NMR (400.14 MHz, THF-d₈,

300 K) δ (ppm) = 7.29 (d, J = 5.20 Hz, 4H), δ = 7.01 (m, 4H), δ = 6.67 (d, J = 8.81 Hz, 4H), δ = 6.14 (t, J = 6.00 Hz, 4H), δ = 5.22 (s, 2H), δ = -1.31 (S, 3H). ^{13}C NMR (100.65 MHz, THF- d_8 , 300 K) δ (ppm) = 156.99, δ = 143.79, δ = 134.58, δ = 122.67, δ = 110.93, δ = 90.77, δ = -2.37. Elemental analysis calcd. (%) for $\text{C}_{23}\text{H}_{21}\text{AlN}_4$: C 72.60, H 5.56, N 14.73; found: C 72.39, H 5.70, N 14.35.

9a: 8 (300 mg, 0.79 mmol) was dissolved in CH_2Cl_2 (5 ml) and a solution of $\text{B}(\text{C}_6\text{F}_5)_3$ (404 mg, 0.79 mmol) in CH_2Cl_2 (5 ml) was added by syringe at ambient temperature. The solution was stirred for 2 h at ambient temperature and the solvent was evaporated under vacuum. The residue was washed with hexane (1x 10 ml) to afford **9a** as an orange powder (580 mg, 82 %). ^1H NMR (400.14 MHz, CD_2Cl_2 , 300 K) δ (ppm) = 7.40 (m, 4H), δ = 7.31 (d, J = 6.40 Hz, 4H), δ = 7.09 (d, J = 8.81 Hz, 4H), δ = 6.55 (td, J = 6.80, 1.2 Hz, 4H), δ = 5.63 (s, 2H), δ = 0.46 (S, 3H). ^{13}C (partial) NMR (100.65 MHz, CD_2Cl_2 , 300 K) δ (ppm) = 154.41, δ = 149.57, δ = 147.14, δ = 138.27, δ = 137.24, δ = 136.24, δ = 135.17, δ = 124.80, δ = 113.40, δ = 90.60. ^{11}B NMR (128.38 MHz, CD_2Cl_2 , 300 K) δ (ppm) = -14.94. ^{19}F NMR (376.47 MHz, CD_2Cl_2 , 300 K) δ (ppm) = -133.07, δ = -165.29, δ = -167.90. Elemental analysis calcd. (%) for $\text{C}_{41}\text{H}_{21}\text{AlBF}_{15}\text{N}_4$: C 55.18, H 2.37, N 6.28; found: C 53.71, H 3.12, N 5.53.

9b: 8 (135 mg, 0.35 mmol) was dissolved in CH_2Cl_2 (5 ml) and a solution of $\text{B}(\text{C}_6\text{H}_5)_3$ (86 mg, 0.35 mmol) in CH_2Cl_2 (5 ml) was added by syringe at ambient temperature. The solution was stirred for 2 h at ambient temperature and the solvent was evaporated under vacuum. The residue was washed with hexane (1x 10 ml) to afford **9b** as an orange powder (135 mg, 61 %). ^1H NMR (300.13 MHz, CD_2Cl_2 , 293 K) δ (ppm) = 7.65 – 6.80 (several m, 31H), δ = 5.33 (s, 2H), δ = 0.27 (q, J = 4.08 Hz, 3H). ^{13}C (partial) NMR (75.48 MHz, CD_2Cl_2 , 293 K) δ (ppm) = 139.77, δ = 137.57, δ = 135.77, δ = 133.75, δ = 128.74, δ = 127.10, δ = 126.62, δ = 125.06, δ = 122.97, δ = 120.89. ^{11}B NMR (96.29 MHz, CD_2Cl_2 , 294 K) δ (ppm) = -11.51. Elemental analysis calcd. (%) for $\text{C}_{41}\text{H}_{42}\text{AlBN}_4$: C 78.34, H 6.73, N 8.91; found: C 78.67, H 5.83, N 8.19.

4j: Method a: 9a (200 mg, 0.22 mmol) was dissolved in CH_2Cl_2 (10 ml) and a solution of CoCp^*_2 (74 mg, 0.22 mmol) in CH_2Cl_2 (5 ml) was added by syringe at ambient temperature. The solution was stirred for overnight at ambient temperature after

which the solvent was evaporated under vacuum to afford grayish brown solid residue, which was analyzed by EPR spectroscopy to contain **4j**.

Method b: **9a** (5 mg, 0.022 mmol) and a piece of potassium metal was added in toluene (2 ml) and transferred into an EPR tube. The EPR tube was sonicated for 15 min and the dark red solution was analyzed by EPR spectroscopy to contain **4j**.

Method c: **9b** (80 mg, 0.13 mmol) was dissolved in CH₂Cl₂ (10 ml) and a solution of CoCp₂ (45 mg, 0.13 mmol) in CH₂Cl₂ (5 ml) was added by syringe at ambient temperature. The solution was stirred for overnight at ambient temperature after which the solvent was evaporated under vacuum to afford grayish brown solid residue. Crystallization from CH₂Cl₂:toluene (50:50) mixture afforded the cobaltocenium salt of trisphenylmethylborate as yellow crystals suitable for X-ray analysis (see below).

2. Crystallographic data

Crystallographic data of **8**:

Identification code	shelxl
Empirical formula	C ₂₃ H ₂₁ Al N ₄
Formula weight	380.42
Temperature	173(2) K
Wavelength	0.71073 Å
Crystal system	Monoclinic
Space group	P 21/c
Unit cell dimensions	a = 13.3810(9) Å α = 90°. b = 9.4130(4) Å β = 90.540(2)°. c = 15.6040(10) Å γ = 90°.
Volume	1965.3(2) Å ³
Z	4
Density (calculated)	1.286 Mg/m ³
Absorption coefficient	0.119 mm ⁻¹
F(000)	800
Crystal size	0.24 x 0.04 x 0.04 mm ³
Theta range for data collection	2.96 to 24.99°.
Index ranges	-15 ≤ h ≤ 15, -11 ≤ k ≤ 11, -18 ≤ l ≤ 18
Reflections collected	5851
Independent reflections	3399 [R(int) = 0.0534]
Completeness to theta = 24.99°	98.3 %
Absorption correction	Semi-empirical from equivalents
Max. and min. transmission	0.9953 and 0.9720
Refinement method	Full-matrix least-squares on F ²
Data / restraints / parameters	3399 / 0 / 261
Goodness-of-fit on F ²	1.058
Final R indices [I > 2σ(I)]	R1 = 0.0739, wR2 = 0.1354
R indices (all data)	R1 = 0.1035, wR2 = 0.1555
Largest diff. peak and hole	0.268 and -0.338 e.Å ⁻³

Crystallographic data of [CoCp₂][Ph₃BMe]:

Identification code	shelxl
Empirical formula	C ₂₉ H ₂₈ B Co

Formula weight	446.25	
Temperature	123(2) K	
Wavelength	0.71073 Å	
Crystal system	orthorhombic	
Space group	Pmn 21	
Unit cell dimensions	a = 11.2305(3) Å	$\alpha = 90^\circ$.
	b = 13.0554(2) Å	$\beta = 90^\circ$.
	c = 15.4758(3) Å	$\gamma = 90^\circ$.
Volume	2269.04(8) Å ³	
Z	4	
Density (calculated)	1.306 Mg/m ³	
Absorption coefficient	0.770 mm ⁻¹	
F(000)	936	
Crystal size	0.15 x 0.2 x 0.3 mm ³	
Theta range for data collection	2.73 to 24.99°.	
Index ranges	0 ≤ h ≤ 13, -15 ≤ k ≤ 0, -18 ≤ l ≤ 18	
Reflections collected	4153	
Independent reflections	4153 [R(int) = 0.0000]	
Completeness to theta = 24.99°	99.4 %	
Refinement method	Full-matrix least-squares on F ²	
Data / restraints / parameters	4153 / 1 / 302	
Goodness-of-fit on F ²	1.169	
Final R indices [I > 2σ(I)]	R1 = 0.0574, wR2 = 0.1450	
R indices (all data)	R1 = 0.0605, wR2 = 0.1476	
Absolute structure parameter	0.74(2)	
Largest diff. peak and hole	2.320 and -0.644 e.Å ⁻³	

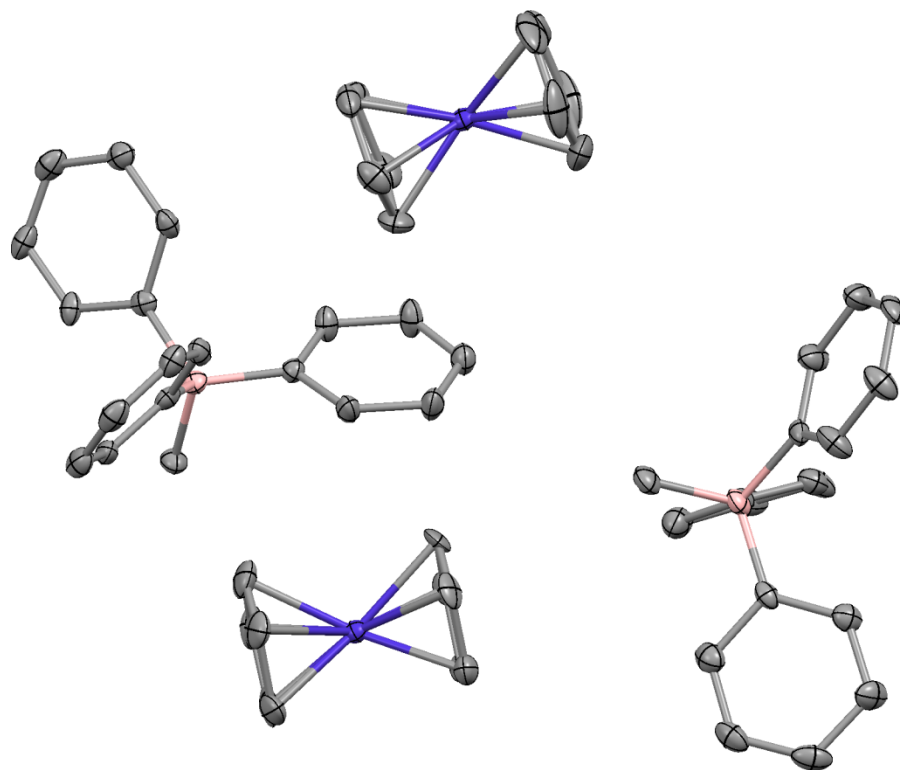


Figure S1. The crystal structure of $[\text{CoCp}_2][\text{Ph}_3\text{BMe}]$ (thermal ellipsoids drawn at 30% probability; hydrogen atoms omitted for clarity).

3. Spectroscopic data

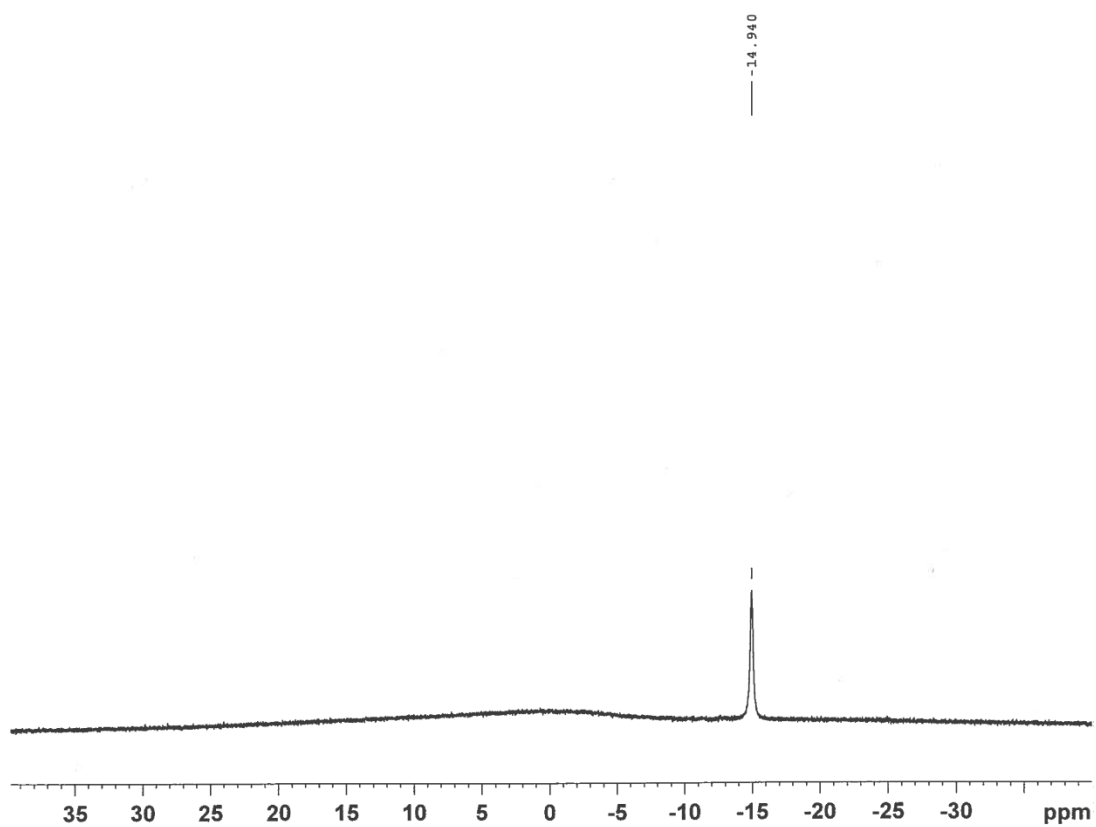


Figure S2. The ^{11}B NMR spectrum of **9a** in CD_2Cl_2 .

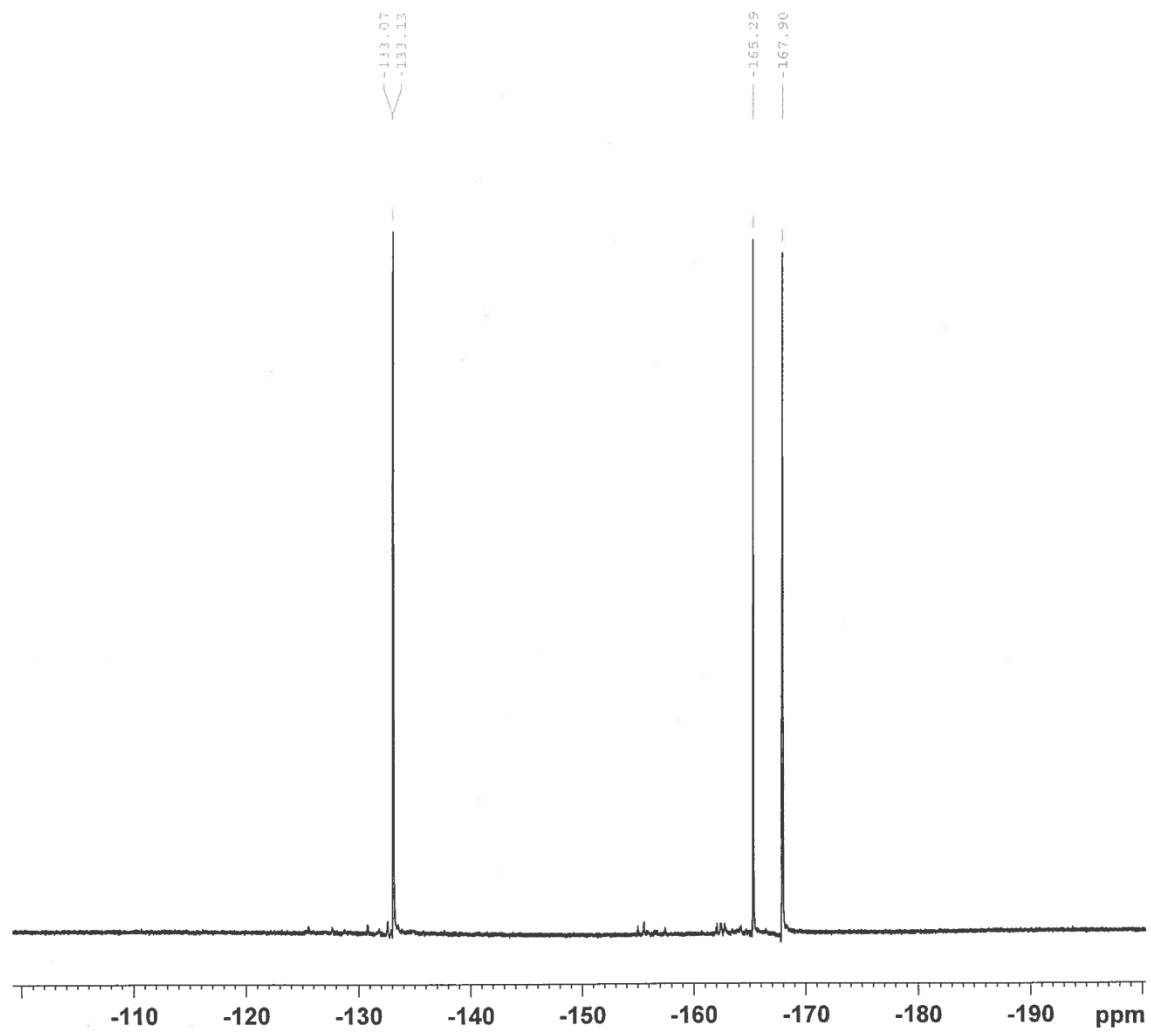


Figure S3. The ^{19}F NMR spectrum of **9a** in CD_2Cl_2 .

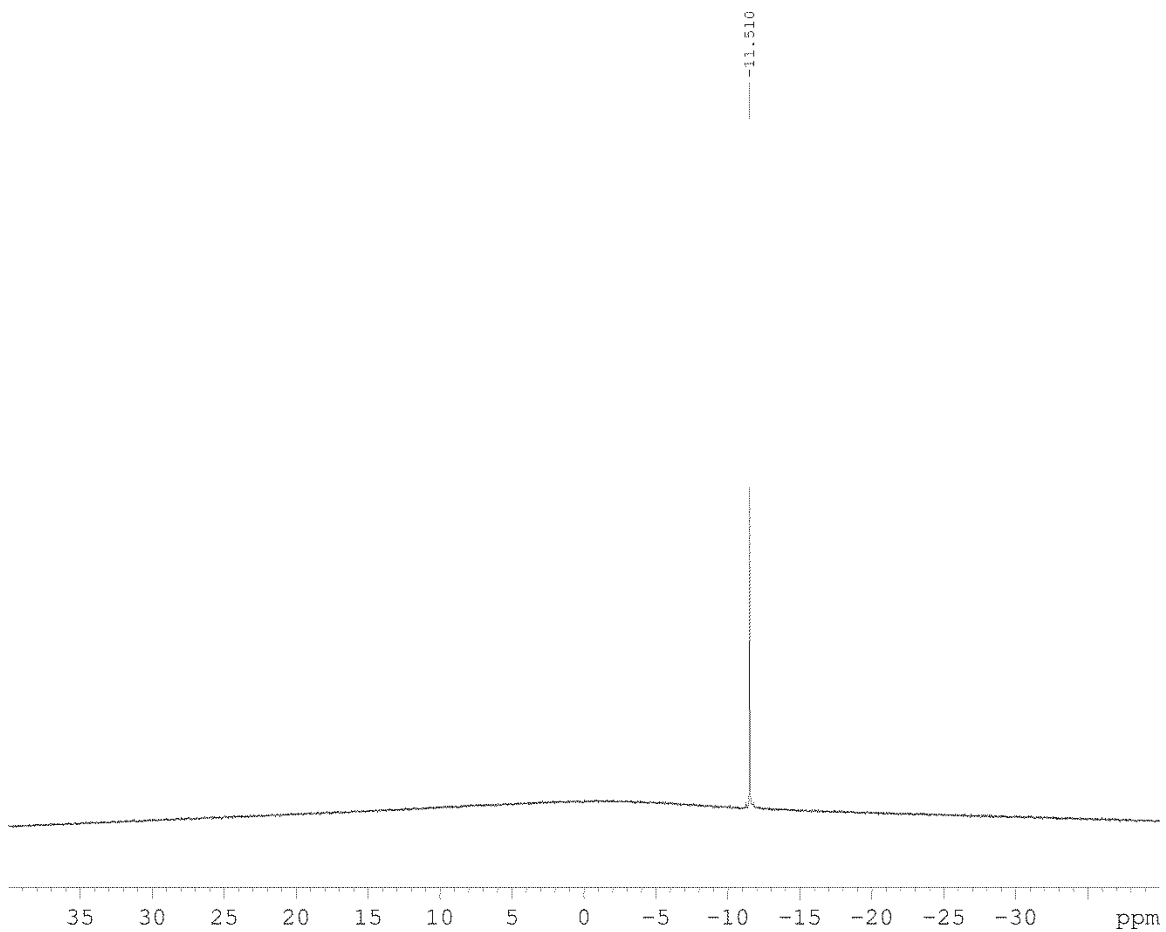


Figure S4. The ^{11}B NMR spectrum of **9b** in CD_2Cl_2 .

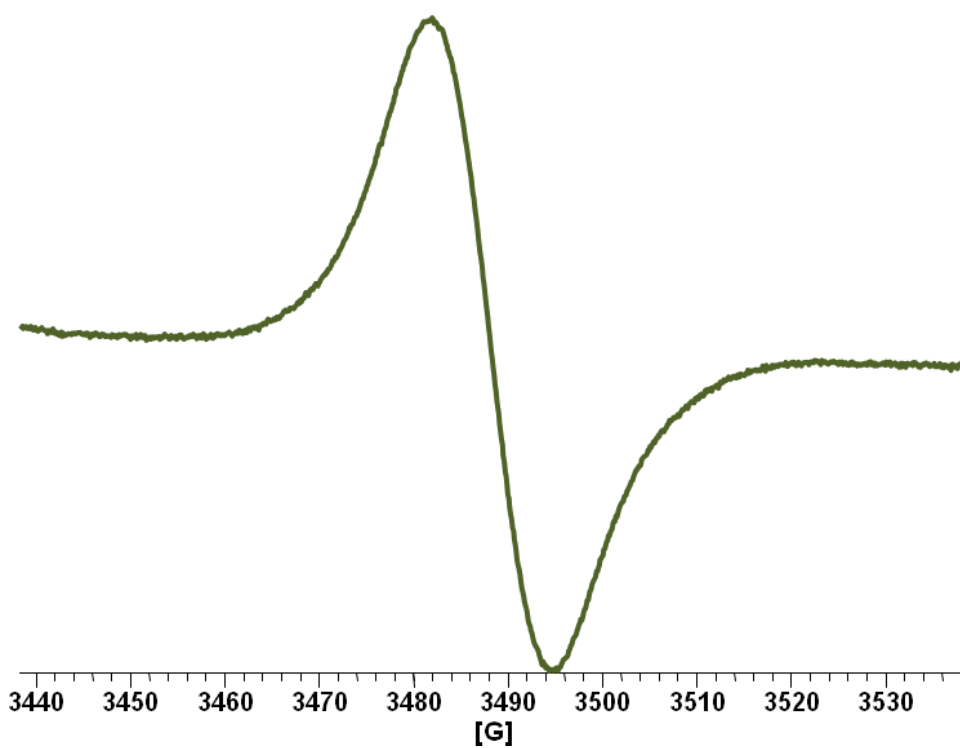


Figure S5. EPR-spectrum of **4j** as obtained from a powder sample ($T = 295$ K, mod.amp. = 1.0 G).

4. Computational details

The structures of radicals **3-6** were optimized by using density functional theory and the PBE1PBE hybrid functional.¹ The calculations used the Ahlrichs' def2-TZVP basis sets;² for indium, the corresponding effective core potential basis set was used. Frequency analyses were performed for optimized geometries to ensure that they correspond to stable minima on the potential energy hypersurface. Calculated spin densities were partitioned to contributions from individual atoms with the help of Mulliken population analysis. All calculations were done with the Turbomole 6.3 and Gaussian 09 program packages.³

¹ (a) J. P. Perdew, K. Burke, M. Ernzerhof, *Phys. Rev. Lett.*, 1997, **78**, 1396; (b) J. P. Perdew, K. Burke, M. Ernzerhof, *Phys. Rev. Lett.*, 1996, **77**, 3865; (c) J. P. Perdew, M. Ernzerhof, K. Burke, *J. Chem. Phys.*, 1996, **105**, 9982; (d) C. Adamo, V. Barone, *J. Chem. Phys.*, 1999, **10**, 6158.

² (a) F. Weigend, R. Ahlrichs, *Phys. Chem. Chem. Phys.*, 2005, **7**, 3297; (b) F. Weigend, M. Häser, H. Patzelt, R. Ahlrichs, *Chem. Phys. Lett.*, 1998, **294**, 143.

³ (a) TURBOMOLE V6.3 2011, a development of University of Karlsruhe and Forschungszentrum Karlsruhe GmbH, 1989-2007, TURBOMOLE GmbH, since 2007; available from <http://www.turbomole.com>. (b) Gaussian 09, Revision A.1, M. J. Frisch, G. W. Trucks, H. B. Schlegel, G. E. Scuseria, M. A. Robb, J. R. Cheeseman, G. Scalmani, V. Barone, B. Mennucci, G. A. Petersson, H. Nakatsuji, M. Caricato, X. Li, H. P. Hratchian, A. F. Izmaylov, J. Bloino, G. Zheng, J. L. Sonnenberg, M. Hada, M. Ehara, K. Toyota, R. Fukuda, J. Hasegawa, M. Ishida, T. Nakajima, Y. Honda, O. Kitao, H. Nakai, T. Vreven, J. A. Montgomery, Jr., J. E. Peralta, F. Ogliaro, M. Bearpark, J. J. Heyd, E. Brothers, K. N. Kudin, V. N. Staroverov, R. Kobayashi, J. Normand, K. Raghavachari, A. Rendell, J. C. Burant, S. S. Iyengar, J. Tomasi, M. Cossi, N. Rega, J. M. Millam, M. Klene, J. E. Knox, J. B. Cross, V. Bakken, C. Adamo, J. Jaramillo, R. Gomperts, R. E. Stratmann, O. Yazyev, A. J. Austin, R. Cammi, C. Pomelli, J. W. Ochterski, R. L. Martin, K. Morokuma, V. G. Zakrzewski, G. A. Voth, P. Salvador, J. J. Dannenberg, S.

Dapprich, A. D. Daniels, Ö. Farkas, J. B. Foresman, J. V. Ortiz, J. Cioslowski, and
D. J. Fox, Gaussian, Inc., Wallingford CT, 2009.

5. Computational data

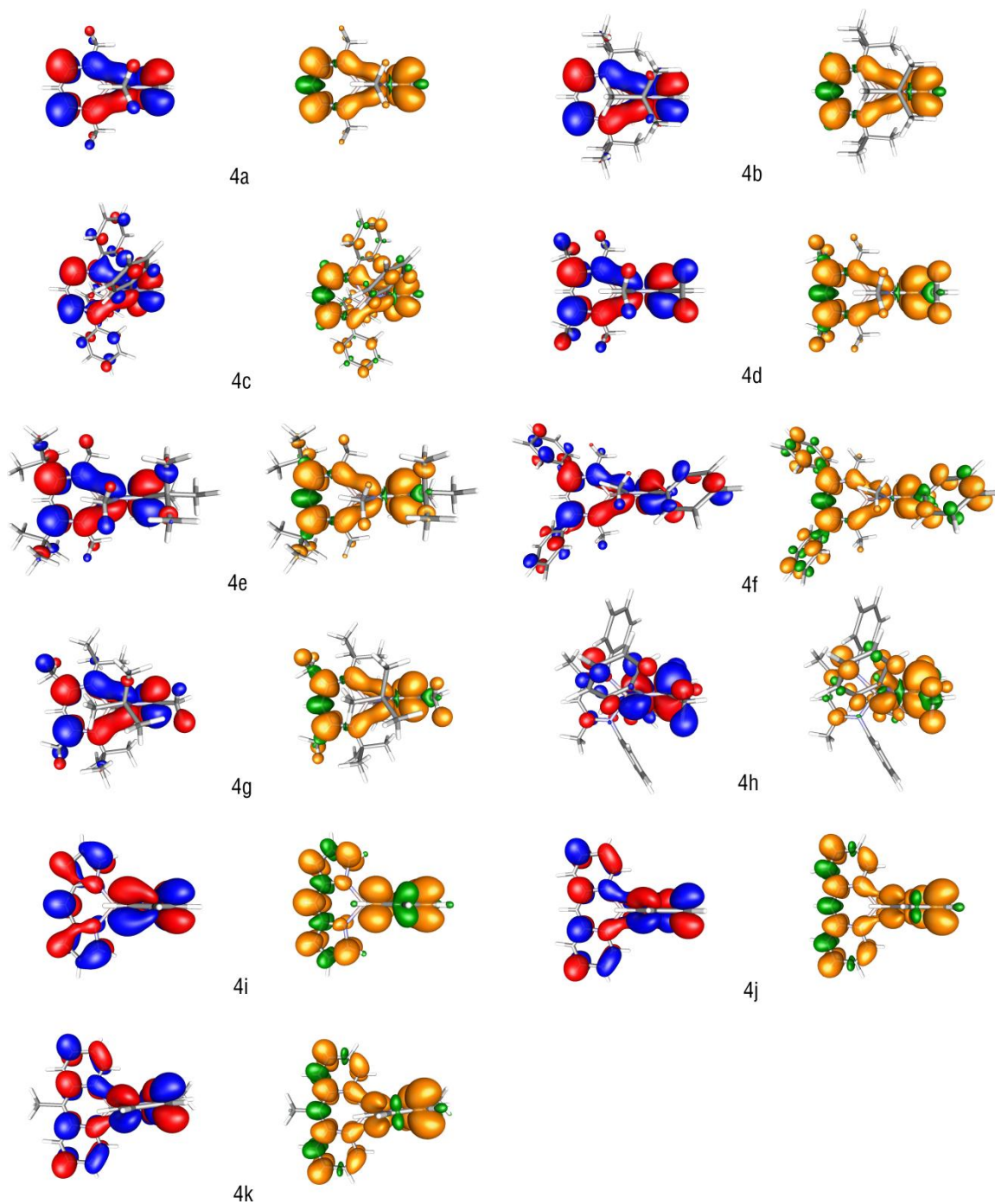


Figure S6. The SOMOs (left) and spin densities (right) of **4a-k**. Colour code: orange = positive spin density, green = negative spin density.

Table S1. Molecular point groups of **3-6**.

	Point group		Point group		Point group		Point group
3a	S_4	4a	D_{2d}	5a	D_{2d}	6a	C_2^a
3b	S_4	4b	D_{2d}	5b	D_{2d}	6b	C_{2v}^a
3c	D_2	4c	D_2	5c	C_2^a	6c	C_2^a
3d	D_{2d}	4d	D_{2d}	5d	D_{2d}	6d	C_1^a
3e	S_4	4e	S_4	5e	C_2^a	6e	C_1^a
3f	D_2	4f	D_2	5f	C_2^a	6f	C_2^a
3g	S_4	4g	S_4	5g	C_2^a	6g	C_2^a
3h	C_2^a	4h	C_2^a	5h	C_2^a	6h	C_2^a
3i	C_s^a	4i	S_4	5i	D_2	6i	D_2
3j	D_{2d}	4j	D_{2d}	5j	D_{2d}	6j	D_{2d}
3k	C_2	4k	C_2	5k	C_2	6k	C_2

^{a)} Spin density localized on one ligand only.

Table S2. Mulliken spin densities of **3-6** at the PBE1PBE/def2-TZVP level of theory.

	N ¹ /N ⁵	C ² /C ⁴	C ³	B		N ¹ /N ⁵	C ² /C ⁴	C ³	Ga
3a	0.036	0.288	-0.122	-0.021	5a	0.052	0.258	-0.115	0.009
3b	0.037	0.288	-0.118	-0.026	5b	0.045	0.267	-0.120	0.041
3c	0.017	0.278	-0.112	-0.033	5c	0.003 / 0.044	0.068 / 0.427	-0.029 / -0.188	0.019
3d	0.030	0.274	-0.126	-0.015	5d	0.049	0.243	-0.116	0.019
3e	0.031	0.290	-0.138	-0.057	5e	0.001 / 0.092	0.032 / 0.470	-0.014 / -0.231	0.014
3f	0.037	0.217	-0.107	-0.022	5f	0.098 / 0.006	0.329 / 0.035	-0.173 / -0.015	0.009
3g	0.036	0.270	-0.128	-0.024	5g	0.083 / 0.003	0.413 / 0.083	-0.211 / -0.039	0.050
3h	0.002 / 0.016	0.064 / 0.457	-0.025 / -0.219	-0.002	5h	0.035 / -0.001	0.474 / 0.011	-0.233 / -0.004	0.026
3i	0.023 / 0.001	-0.158 / 0.002	0.568 / 0.002	0.008	5i	0.016	-0.080	0.291	0.003
3j	0.051	0.157	-0.101	-0.003	5j	0.066	0.145	-0.099	0.007
3k	0.050	0.153	-0.098	0.001	5k	0.066	0.149	-0.095	0.006

Table S2. Continued.

	N ¹ /N ⁵	C ² /C ⁴	C ³	Al		N ¹ /N ⁵	C ² /C ⁴	C ³	ln
4a	0.039	0.267	-0.116	0.034	6a	0.001 / 0.124	0.012 / 0.488	-0.005 / -0.220	-0.003
4b	0.034	0.258	-0.120	0.064	6b	0.112 / 0.004	0.465 / 0.043	-0.213 / -0.020	0.019
4c	0.017	0.257	-0.109	0.045	6c	0.054 / -0.001	0.473 / 0.008	-0.212 / -0.004	0.007
4d	0.036	0.251	-0.117	0.041	6d	0.109 / 0.004	0.442 / 0.029	-0.215 / -0.014	0.009
4e	0.034	0.258	-0.120	0.032	6e	0.103 / -0.003	0.489 / 0.002	-0.243 / 0.000	0.020
4f	0.040	0.196	-0.095	0.039	6f	0.000 / 0.111	0.002 / 0.355	0.000 / -0.189	0.007
4g	0.032	0.256	-0.124	0.074	6g	0.109 / -0.003	0.465 / 0.013	-0.243 / -0.006	0.026
4h	-0.003 / 0.027	0.029 / 0.467	-0.011 / -0.227	0.041	6h	0.039 / 0.000	0.466 / 0.001	-0.230 / 0.001	0.028
4i	0.014	-0.081	0.289	0.006	6i	0.017	-0.078	0.292	0.002
4j	0.057	0.148	-0.098	0.027	6j	0.070	0.143	-0.100	0.004
4k	0.056	0.152	-0.096	0.025	6k	0.051	0.024	-0.001	0.777